

# Comparative study of the crystal field effects in rare earth oxynitrates

Jorma Hölsä<sup>a</sup>, Maarit Karppinen<sup>b</sup> and Eija Kestilä<sup>a,\*</sup>

<sup>a</sup>University of Turku, Department of Chemistry, FIN-20500 Turku (Finland)

<sup>b</sup>Helsinki University of Technology, Department of Chemical Engineering, FIN-02150 Espoo (Finland)

## Abstract

The photoluminescence spectra of the lanthanum and gadolinium oxynitrates doped with  $\text{Eu}^{3+}$ ,  $\text{REONO}_3:\text{Eu}^{3+}$  (RE=La and Gd) were measured at 77 and 300 K. The  ${}^7\text{F}_J$  ( $J=0-5$ ) energy level schemes for the  $4f^6$  electron configuration were simulated by a  $C_{2v}$  phenomenological crystal field (CF). The nine non-zero CF parameters for the  $C_{2v}$  site symmetry reproduce the experimental energy level schemes with rms deviations of 7 and  $5\text{ cm}^{-1}$  for the  $\text{LaONO}_3$  and  $\text{GdONO}_3$  hosts, respectively. The CF effect is stronger in the lanthanum host although otherwise the CF parameters for the two oxynitrate hosts differ only slightly. The  $B_2^k$  ( $k=2, 4$  and  $6$ ) values are low indicating only a slight deviation from a higher  $C_{4v}$  symmetry. The  $B_0^2$ ,  $B_0^4$  and  $B_4^4$  parameters assume high values which are similar to those obtained previously for the other RE oxy compounds, *i.e.* oxyhalides, oxysulfates, oxymolybdates, and oxytungstates. The sixth rank parameters deviate considerably from those obtained for the other RE oxy compounds.

## 1. Introduction

The existence of the RE oxynitrates has been known since the late 1950s [1,2], but the low stability of these compounds has hindered the characterization of even their most elementary properties. No wonder that the structure of oxynitrates is largely contested and has been subject to several contradictory reports [3–8]. The optical study of the  $\text{Eu}^{3+}$  doped lanthanum oxynitrate [9], however, suggests that the crystal structure of the oxynitrates is related to the common rare earth oxy compounds with tetragonal symmetry [10].

The RE oxy compounds resemble the corresponding bismuthyl compounds and hence correspond to a general formula  $(\text{REO})_n\text{X}$  [11] where X can be almost any simple or complex anion. Similar to the RE oxynitrates, the crystal structure of the simple  $\text{BiONO}_3$  [12] has also not been resolved to date. Extensive spectroscopical studies on the RE oxy compounds have revealed a similar luminescence behavior within this group, *i.e.* oxyhalides, oxymolybdates, oxytungstates, oxycarbonates and oxysulfates [13–17]. The  $(\text{REO})_n^{n+}$  entity seems to be responsible to a large extent for all the luminescence properties of these compounds.

The present paper reports the results of the phenomenological simulation of the CF splitting of the  ${}^7\text{F}_J$  ( $J=0-5$ ) levels of the  $\text{Eu}^{3+}$  ion in both the  $\text{LaONO}_3$

and  $\text{GdONO}_3$  host in order to supplement the previous investigation of the luminescence properties of the lanthanum oxynitrate doped with trivalent europium [9].

## 2. Experimental details

### 2.1. Sample preparation

The RE oxynitrates,  $\text{REONO}_3$  (RE=La and Gd) were obtained in powder form by the thermal decomposition of the RE nitrate hydrates or the RE ammonium double nitrate hydrates. The  $\text{REONO}_3$  phases are hardly stable above 400 K [1,2,18–20], and thus the initial materials were heated only for 1 h at 620 and 530 K for  $\text{LaONO}_3$  and  $\text{GdONO}_3$ , respectively. The routine X-ray diffraction analysis revealed no presence of other than the oxynitrate phase in the final products. A small amount of  $\text{Eu}^{3+}$  (from 1 up to 5 mol%) was used as a dopant for optical measurements.

### 2.2. Spectroscopic measurements

The photoluminescence spectra of the  $\text{REONO}_3:\text{Eu}^{3+}$  powder samples were recorded both at 300 and 77 K. Either the global UV radiation from a 150-W mercury lamp around 300 nm or the blue line (457.9 nm) of the argon ion laser (to excite the  ${}^5\text{D}_2$  level) were utilized. Selective excitation on the  ${}^5\text{D}_0$  level was carried out by a Spectra Physics 375/376

\*Author to whom correspondence should be addressed.

continuous wave rhodamine 6G dye laser (linewidth  $0.7 \text{ cm}^{-1}$ ) pumped by a Spectra Physics 164 cw argon ion laser. The luminescence was dispersed by a 1-m Jarrell-Ash monochromator and detected by a Hamamatsu R928 photomultiplier. The overall resolution of the setup was better than  $1.0 \text{ cm}^{-1}$ . The  ${}^5\text{D}_{0-2} \rightarrow {}^7\text{F}_{0-5}$  transitions between 480 and 775 nm were considered in detail for the  $\text{LaONO}_3$  host. However, only the  ${}^5\text{D}_{0,1} \rightarrow {}^7\text{F}_{0-5}$  transitions between 580 and 775 nm could be detected for  $\text{GdONO}_3$ .

### 2.3. Crystal structure of RE oxynitrates

The earlier reports [3–7] based on the results of the X-ray powder diffraction [3] and IR and Raman spectroscopic investigations [7] have assigned the crystal structure of RE oxynitrates to the cubic system. The most recent studies by Hajek *et al.* [8] have associated their structure with the tetragonal system. The cubic structure seems to be oversimplified, while the tetragonal one is in good agreement with that of the oxyhalides, for instance. The exact crystal structure of the RE oxynitrates remains still largely unknown although a set of approximate coordinates for the atoms belonging to the  $(\text{REO})_n^{3+}$  entity have been obtained [8]. From the data available, one can rather safely suppose that the RE oxynitrates form a structurally isomorphous series.

### 2.4. Crystal field model

The strong luminescence of the  $\text{Eu}^{3+}$ -ion in the visible range is due to the exceptionally large energy gap between the emitting  ${}^5\text{D}$ -levels,  ${}^5\text{D}_{0-4}$  and the ground  ${}^7\text{F}_{0-6}$  septet [13]. The phenomenological simulation of the  $4f^6$  electron configuration equally profits from this theoretical and energetic isolation of the  ${}^7\text{F}_7$  ground multiplet. The free-ion terms of the total Hamiltonian, easily adding up to some 15 parameters, can hence be discarded in the term  $H_{\text{CF}}$ . The CF term incorporates only the effects of the non-spherical interactions arising from the surrounding charges on the 4f-electrons of the  $\text{RE}^{3+}$ -ion.

The complete energy level scheme of the  $4f^6$  configuration consists of 3003 individual Stark components. The subsequent calculations should hence employ a diagonalization of a square matrix of size  $3003 \times 3003$ . While using only the  ${}^7\text{F}_{0-6}$  multiplet, the whole treatment can be reduced to a  $49 \times 49$  matrix easily carried out on an ordinary PC [21]. Further simplifications can be achieved by splitting the matrix into submatrices according to the appropriate symmetry of the  $\text{RE}^{3+}$  site.

Following the formalism of Wybourne [22], the CF Hamiltonian can be written in a general form for any  $4f^N$  (or  $nd^N$ ) electron configuration as follows:

$$H_{\text{CF}} = \sum_{k=0}^{\leq 6} \sum_{q \geq k}^{\leq k} \sum_{i=1}^N [B_q^k(C_q^k(i) + (-1)^q C_{-q}^k(i)) + iS_q^k(C_q^k(i) - (-1)^q C_{-q}^k(i))]$$

This expression includes the spherical tensors  $C_q^k$  of rank  $k$ ,  $B_q^k$  and  $S_q^k$  as the real and imaginary CF parameters, respectively. These parameters are usually fitted from experiments since their evaluation from theoretical considerations is usually not feasible. The actual fitting procedure utilized the standard least squares calculations to optimize the  $B_q^k$  parameters. The root mean square deviation  $\sigma$  between the experimental and calculated energy level values was used as a figure of merit to describe the quality of the simulation.

## 3. Results and discussion

### 3.1. Analysis of luminescence spectra

Under UV excitation, the  $\text{REONO}_3:\text{Eu}^{3+}$  samples emit orange-red light created mainly by the transitions from the lowest excited  ${}^5\text{D}$  level,  ${}^5\text{D}_0$  [13,14]. For the  $\text{LaONO}_3$  host, an emission of an order of magnitude weaker was also observed from the higher  ${}^5\text{D}_{1-2}$  levels. The emission spectra of  $\text{REONO}_3:\text{Eu}^{3+}$  are characterized by an intense, usually strictly forbidden  ${}^5\text{D}_0 \rightarrow {}^7\text{F}_0$  transition along with dominating electric dipole transitions  ${}^5\text{D}_0 \rightarrow {}^7\text{F}_2$  and  ${}^5\text{D}_0 \rightarrow {}^7\text{F}_4$ . The magnetic dipole  ${}^5\text{D}_0 \rightarrow {}^7\text{F}_1$  transitions are rather weak. All these common features imply the existence of the  $(\text{REO})_n^{3+}$  complex cation as found for the RE oxyhalides as a representative case of RE oxy compounds.

The total lifting of the  $2J+1$  degeneracy of the  ${}^7\text{F}_{1-5}$  levels as well as the absence of any group-theoretical selection rules implies a  $C_{2v}$  symmetry (at most), clearly lower than the  $C_{4v}$  symmetry in the RE oxyhalides. The 26 and 28 Stark levels (out of a total of 49) form a nearly complete set for the  ${}^7\text{F}_{0-4}$  levels whereas only a few components were obtained for the  ${}^7\text{F}_5$  level and none for the  ${}^7\text{F}_6$  level.

The CF splitting of the  ${}^7\text{F}_{0-5}$  levels is somewhat larger for the  $\text{LaONO}_3$  host in agreement with the trend found for the tetragonal RE oxy compounds [13–15]. Otherwise, the splittings in both  $\text{REONO}_3$  hosts closely resemble each other (Table 1). The nephelauxetic effect for the  ${}^7\text{F}_{0-4}$  levels as shown by the increase in the level energies from the  $\text{GdONO}_3$  to the  $\text{LaONO}_3$  host is due to the difference in the size of the host cation.

### 3.2. Crystal field simulation

The phenomenological CF analysis was initially carried out in  $C_{2v}$  symmetry although the actual symmetry of the  $\text{RE}^{3+}$  site remains unknown. This symmetry was

TABLE 1. The calculated and experimental  ${}^7F_J$  ( $J=0-5$ ) energy level schemes of the  $\text{REONO}_3:\text{Eu}^{3+}$  ( $\text{RE}=\text{La}$  and  $\text{Gd}$ ) for the  $C_{2v}$  symmetry at 77 K (in  $\text{cm}^{-1}$  units)

Level	$\text{LaONO}_3:\text{Eu}^{3+}$		$\text{GdONO}_3:\text{Eu}^{3+}$		
		Obs.	Calc.	Obs.	Calc.
${}^7F_0$	$A_1$	0	0	$A_1$	0
${}^7F_1$	$A_2$	202	195	$A_2$	236
	$B'$	429	433	$B'$	391
	$B''$	512	514	$B''$	494
${}^7F_2$	$B''$	966	956	$B''$	922
	$A_1$	1009	1007	$A_1$	959
	$B'$	1031	1030	$B'$	965
${}^7F_3$	$A_1$	1144	1144	$A_1$	1166
	$A_2$	1329	1338	$A_2$	1321
	$A_2$	1855	1859	$A_2$	1828
	$B'$	1885	1894	$B'$	1898
	$B''$	1939	1937	$B''$	1928
	$B''$	1982	1980	$B''$	1940
${}^7F_4$	$B'$	2009	1997	$B'$	1974
	$A_2$	2041	2042	$A_1$	2046
	$A_1$	2093	2098	$A_2$	2059
	$A_1$	2687	2687	$A_1$	2609
	$A_2$	2769	2774	$B''$	2742
	$B''$		2849	$A_2$	2763
	$B'$	2863	2862	$B'$	2854
	$A_1$	2903	2903	$A_2$	2865
	$A_2$	2932	2931	$A_1$	2908
	$A_1$		2997	$A_1$	2947
${}^7F_5$	$B'$	3005	3003	$B'$	3041
	$B''$	3053	3051	$B''$	3049
	$B''$		3789	$B'$	3759
	$B'$		3793	$B''$	3765
	$A_2$		3937	$A_2$	3863
	$B'$	3959	3954	$B''$	3865
	$A_1$		3964	$A_1$	3877
	$B''$		3994	$B'$	3894
	$A_1$	4021	4022	$A_1$	3966
	$B''$		4169	$A_2$	4051
${}^7F_5$	$A_2$	4180	4170	$B''$	4133
	$B'$		4232	$B'$	4170
	$A_2$		4234	$A_2$	4182

chosen because of the probable symmetry in the partly known  $(\text{REO})_n^{3+}$  entity and also avoids the introduction of the  $S_q^k$  imaginary parameters. Too high number of parameters to be fitted might also render the physical meaning of the parametrization unintelligible. The  $C_{2v}$  symmetry restricts the number of CF parameters to nine:  $B_0^2$ ,  $B_2^2$ ,  $B_0^4$ ,  $B_2^4$ ,  $B_4^4$ ,  $B_0^6$ ,  $B_2^6$ ,  $B_4^6$  and  $B_6^6$  [23].

The  ${}^7F_{0-5}$  levels in  $\text{REONO}_3:\text{Eu}^{3+}$  matrices were successfully simulated as the low rms deviations, 5 and  $7 \text{ cm}^{-1}$ , between the calculated and experimental energy levels show for the  $\text{LaONO}_3$  and  $\text{GdONO}_3$  host, respectively (Table 2). The correctness of the simulation is also revealed by the absence of any individual large discrepancies between the experimental and calculated energy levels (Fig. 1). The two sets of  $B_q^k$  parameters are rather similar although the CF strength parameter

TABLE 2. The evolution of the CF parameters in the  $\text{REONO}_3:\text{Eu}^{3+}$  ( $\text{RE}=\text{La}$  and  $\text{Gd}$ ) series according to the  $C_{2v}$  symmetry (in  $\text{cm}^{-1}$  units)

$B_q^k$	$\text{LaONO}_3:\text{Eu}^{3+}$	$\text{GdONO}_3:\text{Eu}^{3+}$
$B_0^2$	-1149(21)	-878(18)
$B_2^2$	$\mp 133(13)$	$\mp 187(12)$
$B_0^4$	-1005(26)	-1348(23)
$B_2^4$	$\pm 224(35)$	$\mp 17(35)$
$B_4^4$	863(19)	933(16)
$B_0^6$	168(44)	-194(32)
$B_2^6$	$\pm 129(34)$	$\pm 344(26)$
$B_4^6$	165(25)	385(23)
$B_6^6$	$\mp 168(27)$	$\pm 22(25)$
$\sigma$	7	5
Levels	26	28

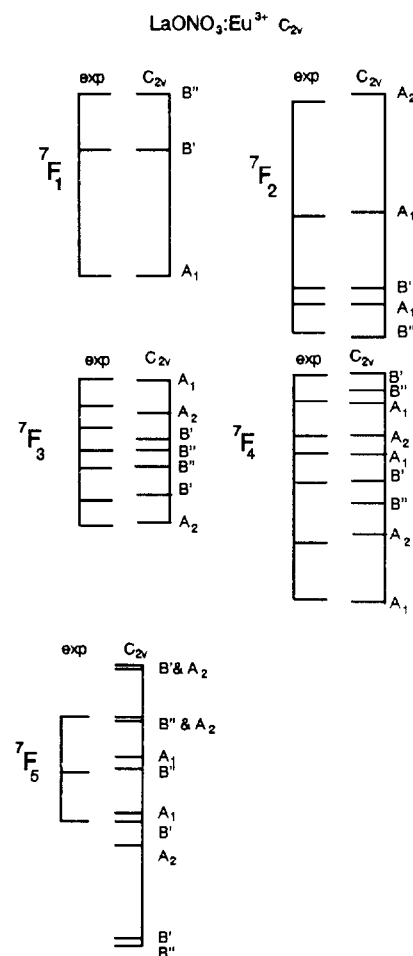


Fig. 1. Comparison between the calculated and experimental CF splitting of the  ${}^7F_{0-5}$  levels of  $\text{LaONO}_3:\text{Eu}^{3+}$  for the  $C_{2v}$  symmetry.

$S$  [24] increases from the  $\text{GdONO}_3$  to the  $\text{LaONO}_3$  host. The distortions from even a higher  $C_{4v}$  symmetry were found to be unimportant in both matrices because the values of the  $B_2^k$  ( $k=2, 4$  and  $6$ ) and  $B_6^6$  parameters are low.

The CF parameter sets are characterized by strong values for the  $B_0^2$ ,  $B_0^4$  and  $B_4^4$  parameters whereas the sixth rank parameters assumed rather low values (Table 2). Hence, the present results are similar to those obtained previously for the other RE oxy compounds, oxyhalides, oxysulfates, oxymolybdates, or oxytungstates [13–17], as far as the second and fourth rank parameters are concerned. In comparison, the  $B_q^k$  set obtained for LaOCl:Eu<sup>3+</sup> is as follows:  $B_0^2 = -1281$ ,  $B_0^4 = -467$ ,  $B_4^4 = \pm 1036$ ,  $B_0^6 = 582$ , and  $B_4^6 = \pm 334 \text{ cm}^{-1}$  [13]. The sixth rank parameters, however, deviate considerably from the results for LaOCl:Eu<sup>3+</sup>.

The reasons for the differences between these two RE oxy compounds can be due to either the origin of the parameters, or the nature of the compounds themselves. To begin with, the origin of the parameters, the second (and fourth) rank parameters describe the short range effects, which, for the RE oxy compounds, correspond to those within the (REO)<sub>n</sub><sup>3+</sup> entity [13]. The sixth rank parameters, on the other hand, reflect the long range effects associated with the NO<sub>3</sub><sup>-</sup> groups. Moreover, because the nitrate group differs considerably from the typical anions for the tetragonal RE oxy compounds, the halides, one should be careful in making too general conclusions, especially when the exact crystal structure of the RE oxynitrates remains unknown. The unsuccessful efforts to carry out the structure analysis might indicate some kind of structural disorder, especially in the nitrate positions which complicates the analysis even more. Hence, it is concluded that only the determination of the exact crystal structure of RE oxynitrates can resolve the differences observed.

### Acknowledgments

Financial support from the Academy of Finland (project no. 4966) to the authors (J.H. and E.K.) is gratefully acknowledged. The authors are indebted to

Dr. P. Porcher (U.P.R. 209, C.N.R.S., France) for the use of the luminescence equipment and the matrix diagonalization program.

### References

- 1 W.W. Wendlandt, *Anal. Chim. Acta*, **15** (1956) 435.
- 2 W.W. Wendlandt and J.L. Bear, *J. Inorg. Nucl. Chem.*, **12** (1960) 276.
- 3 M. Daire and P. Lehuède, *C.R. Acad. Sci. (Paris) Ser. C*, **270** (1970) 1407.
- 4 B. Hajek, E. Holeckova and J. Ondracek, *Sb. Vys. Sk. Chem.-Technol. Prazé, Anorg. Chem. Technol.*, **B30** (1984) 115.
- 5 B. Hajek and E. Holeckova, *Tento Sb.*, **B18** (1974) 73.
- 6 J.-C.G. Bünzli, B. Klein and V. Kaspárek, *J. Less-Common Met.*, **93** (1983) 157.
- 7 J.-C.G. Bünzli, E. Moret and J.R. Yersin, *Helv. Chim. Acta*, **61** (1978) 762.
- 8 B. Hajek and E. Holeckova, *Sb. Vys. Sk. Chem.-Technol. Prazé, Anorg. Chem. Technol.*, **B25** (1980) 97.
- 9 J. Hölsä and M. Karppinen, *Eur. J. Solid State Inorg. Chem.*, **28** (1991) 135.
- 10 P. Caro, *J. Less-Common Met.*, **16** (1968) 367.
- 11 P. Caro, *C.R. Acad. Sci. (Paris) Ser. C*, **262** (1966) 992.
- 12 G. Kiel and G. Gattow, *Naturwissenschaften*, **55** (1968) 389.
- 13 J. Hölsä and P. Porcher, *J. Chem. Phys.*, **75** (1981) 2108.
- 14 J. Hölsä and P. Porcher, *J. Chem. Phys.*, **76** (1982) 2790.
- 15 P. Porcher, D.-R. Svoronos, M. Leskelä and J. Hölsä, *J. Solid State Chem.*, **46** (1983) 101.
- 16 J. Huang, J. Lories and P. Porcher, *J. Solid State Chem.*, **43** (1982) 87.
- 17 O.-K. Moune-Minn and P. Caro, *J. Crystallogr. Spectrosc. Res.*, **12** (1982) 153.
- 18 K.C. Patil, R.K. Gosani and C.N.R. Rao, *Inorg. Chim. Acta*, **1** (1967) 155.
- 19 M. Karppinen, P. Kyläkoski, L. Niinistö and C. Rodellas, *J. Therm. Anal.*, **35** (1989) 347.
- 20 J.M. Haschke, *Inorg. Chem.*, **13** (1974) 13.
- 21 P. Porcher, Computer programs REEL and IMAGE for the simulation of d<sup>N</sup> and f<sup>N</sup> configurations involving the real and imaginary crystal field parameters, 1989, unpublished.
- 22 B.G. Wybourne, *Spectroscopic Properties of Rare Earths*, Interscience, New York, 1965.
- 23 J.L. Prather, *NBS Monogr. (US)*, **19** (1961).
- 24 N.C. Chang, J.B. Gruber, R.P. Leavitt and C.A. Morrison, *J. Chem. Phys.*, **76** (1982) 3877.